Meccanica (2016) 51:1897–1911
DOI 10.1007/s11012-015-0343-5

A novel integration scheme for solution of consistent mass matrix in free and forced vibration analysis

Gang Yang · Dean Hu · Guowei Ma · Detao Wan

Received: 1 September 2015 / Accepted: 1 December 2015 / Published online: 12 December 2015

Abstract The solution of mass matrix is one of the important parts for dynamic analysis of finite element method (FEM). In general FEM procedure, the numerical integration of consistent mass matrix needs to carry out the same operation as the stiffness matrix, which includes the coordinate mapping and computing of Jacobian matrix. There has been proposed smoothed finite element method for evaluating stiffness matrix to avoid the coordinate mapping and computing of Jacobian matrix in the numerical integration. In this work, a novel integration scheme is proposed to calculate the consistent mass matrix, in which a symbolic integration is implemented by combining indefinite integral with Gauss divergence theorem. Then, the novel integration scheme of consistent mass matrix is incorporated with the smoothing strain technique for free and forced vibration analysis. The accuracy and the convergence properties of the present method are investigated by several numerical examples. It can be concluded from the numerical results that the present method is robust and stability for dynamic analysis.

Keywords Vibration problems · Consistent mass matrix · Symbolic integral · Gauss divergence theorem · SFEM

G. Yang · D. Hu (✉) · D. Wan
State Key Laboratory of Advanced Design and Manufacturing for Vehicle Body, College of Mechanical and Vehicle Engineering, Hunan University, Changsha 410082, People's Republic of China
e-mail: hudean@hnu.edu.cn

G. Yang · G. Ma
School of Civil, Environmental and Mining Engineering, The University of Western Australia, Crawley, Perth, WA 6009, Australia

1 Introduction

Dynamic problems exist in a broad field of applied science and engineering, such as motor with high speed rotation, centrifugal compressor and aircraft, their structural responses are produced by inertia effect and dynamic load. Due to the limitations of analytical methods, the finite element method (FEM) has become one of the most popular numerical approaches for analysis of structure dynamic problems. Generally, the dynamic equations of FEM include stiffness matrix, mass matrix, damping matrix and force vector, which obtained from the equilibrium formulations and discretization techniques [1]. However, because of the Gauss integration with coordinate mapping and computing of Jacobian matrix, the computational accuracy of FEM can be significantly decreased when the elements are severely irregular or heavily distorted.

In order to overcome the limitations of traditional FEM, the smoothed FEM (SFEM) has been proposed [2], which is formulated by incorporating the strain smoothing technique of mesh-free methods [3] into

the framework FEM. In the strain smoothing process of SFEM, the coordinate mapping is not required and only shape function itself is involved in computing the field gradients. Compared with the traditional FEM, the SFEM can yield more accurate results even for the extremely irregular meshes. Based on the division of smoothing integral domain, a series of SFEM models have been proposed, such as the celled-based SFEM (CS-FEM) [2, 4, 5], node-based SFEM (NS-FEM) [6, 7], edge-based SFEM [8–10] and so on. Many engineering problems have been employed by the application of SFEM, including the analysis of plate [11], shell [12], cracking [13, 14], free and forced vibration problems [15, 16], etc. However, the SFEM can not completely avoid the coordinate mapping when the formulation of finite element matrix is associated with shape function without partial derivative, such as the consistent mass matrix and damping matrix in dynamic analysis. Thus, it should be significant if the consistent mass matrix and damping matrix can be obtained as the same with the smoothing strain matrix to avoid the coordinate mapping.

Generally, there are two ways to construct mass matrix, i.e., the consistent mass matrix and the lumped mass matrix. For the consistent mass matrix, the same displacement model is used for deriving stiffness matrix and mass matrix. The lumped mass matrix, which is obtained by concentrated mass at the degree of freedom (DOF) of nodes, is diagonal and independent of shape function. Generally, the lumped mass matrices overestimate the mass effect and hence give lower natural frequencies than the exact ones [17]. On the other hand, the underestimation of consistent mass matrices causes higher natural frequencies. But under certain conditions, the same accuracy can be achieved by two kinds of mass matrices [18, 19]. However, the lumped mass matrix has higher computational efficiency than consistent mass matrix, and the consistent mass matrix has higher convergence rate than lumped mass matrix for both eigenvalue and eigenfunction in dynamic analysis [18, 20]. Furthermore, it should be noted that the lumped mass matrix is conditionally used [18]. When the high-order interpolation is used or high-order eigenproblem is involved in analysis, the accuracy of results obtained by lumped mass matrix should decrease compared with that given by consistent mass matrix [18]. In this paper, the consistent mass matrix is employed for dynamic analysis and a novel integration scheme is adopted to solve the consistent mass matrix.

In order to accurately compute the integration of function for an arbitrary domain without coordinate mapping, an integration technique by using symbolic integration combined indefinite integral with Gauss divergence theorem is proposed [21, 22]. In the proposed integration technique [21], the domain integral can be reduced to boundary integral as the integrand function is known a priori. For two-dimensional (2D) problems, the domain integral is converted to boundary integral along the boundary lines, and the Gaussian quadrature on each linear segment of boundary can achieve good accuracy even though severely irregular or heavily distorted elements are used. Obviously, the integration for consistent mass matrix of FEM is related to a pre-defined shape function and hence it can be evaluated by using the symbolic integration combined indefinite integral with Gauss divergence theorem.

In this paper, the novel integration scheme of consistent mass matrix is incorporated into the CS-FEM for solving the free and forced vibration problems. The present integration scheme is also adopted for constant damping matrix which has the similar formulation as consistent mass matrix. The performances of the present method are demonstrated by several numerical examples including the models under extremely irregular meshes.

2 Symbolic integration combining indefinite integral with Gauss divergence theorem

The symbolic integration combining indefinite integral with Gauss divergence theorem is briefed introduced [21] in this section. One crucial step of FEM is that numerical calculation of the following integral

$$\int_{\Omega} f(\mathbf{x})\mathrm{d}\Omega \tag{1}$$

where $f(\mathbf{x})$ is generic function defined over an arbitrary domain Ω.

The integral formulation (1) can be rewritten as a scalar form in three-dimensional coordinate system (x, y, z)

$$\int_{V} f(x, y, z)\mathrm{d}V \tag{2}$$

where V is the integral volume. In order to implement the divergence theorem, a vector $\hat{\psi}(x, y, z)$ is constructed, which satisfies

$$f = \mathrm{div}\hat{\psi} \tag{3}$$

where

$$\hat{\psi} = \varphi_1 \hat{\imath}_1 + \varphi_2 \hat{\imath}_2 + \varphi_3 \hat{\imath}_3 \tag{4}$$

The components φ_1, φ_2 and φ_3 are assumed to be integrable everywhere within the volume V. $\hat{\imath}_1$, $\hat{\imath}_2$ and $\hat{\imath}_3$ are the unit vectors along the coordinate directions x, y, z, respectively.

Substituting Eq. (3) into Eq. (2), and applying the Gauss divergence theorem, leads to

$$\begin{aligned}\int_V \mathrm{div}\hat{\psi}\mathrm{d}V &= \int_S \hat{\psi}\cdot\hat{n}\mathrm{d}S \\ &= \int_S (\varphi_1 n_1 + \varphi_2 n_2 + \varphi_3 n_3)\mathrm{d}S\end{aligned} \tag{5}$$

where S is the boundary surface of volume V. $\hat{n} = n_1\hat{\imath}_1 + n_2\hat{\imath}_2 + n_3\hat{\imath}_3$ is the outward normal on S.

In order to satisfy $f = \mathrm{div}\hat{\psi}$, that

$$\varphi_2 = \varphi_3 = 0 \tag{6}$$

and

$$\varphi_1(x,y,z) = \int f(x,y,z)\mathrm{d}x + c(y,z) \tag{7}$$

where $c(y,z)$ is an arbitrary function independent of x. It has been proved in the Ref. [21] that

$$\int_S c(y,z)n_1\mathrm{d}S = 0 \tag{8}$$

Then, the volume integral in Eq. (2) can be rewritten as

$$\int_V f(x,y,z)\mathrm{d}V = \int_S \left(\int f(x,y,z)dx\right)n_1\mathrm{d}S \tag{9}$$

It can be seen from Eq. (9) that the volume integral in Eq. (2) has been reduced to surface integral with the indefinite integral.

According to the similar process, the domain integral of generic function $f(x,y)$ in plane coordinate system (x,y) can be given as

$$\int_S f(x,y)\mathrm{d}S = \int_\Gamma \left(\int f(x,y)\mathrm{d}x\right)n_1\mathrm{d}\Gamma \tag{10}$$

in which Γ is the boundary of integral domain. If the integral domain includes k-sides, the boundary of integral domain in Eq. (10) is piecewise smooth and continuous, thus the boundary integral can be written as the sum of the integrals on the individual side $\Gamma_i (i = 1, 2, \cdots, k)$ of the integral domain

$$\int_S f(x,y)\mathrm{d}S = \sum_{i=1}^{k}\int_{\Gamma_i}\left(\int f(x,y)\mathrm{d}x\right)n_1^i\mathrm{d}\Gamma \tag{11}$$

where n_1^i is the cosine of angle between outward normal on Γ_i and x. The integral of Eq. (11) can be calculated by analytical integral or numerical integral with Gaussian quadrature.

The surface integral has been recast into line integral through Eq. (11). When the Gaussian quadrature is implemented, Eq. (11) can be calculated by the following equation

$$\int_S f(x,y)\mathrm{d}S = \sum_{i=1}^{k}\sum_{j=1}^{N_G}\frac{1}{2}w_{i,j}\varphi_1\left(x_{i,j}^{GP}, y_{i,j}^{GP}\right)n_1^i l_i \tag{12}$$

and

$$\varphi_1\left(x_{i,j}^{GP}, y_{i,j}^{GP}\right) = \left(\int f(x,y)\mathrm{d}x\right)\Big|_{\left(x_{i,j}^{GP}, y_{i,j}^{GP}\right)} \tag{13}$$

where $\left(x_{i,j}^{GP}, y_{i,j}^{GP}\right)$ is the integral point of boundary segment of Γ_i, whose length is denoted as l_i. $w_{i,j}$ is the weight corresponding to Gaussian integral point $\left(x_{i,j}^{GP}, y_{i,j}^{GP}\right)$. N_G is the number of integral points on each boundary segment Γ_i.

3 The novel integration scheme for consistent mass matrix

The symbolic integration introduced in Sect. 2 is developed to establish a novel integration scheme for consistent mass matrix of plane stress problems. Generally, the consistent mass matrix $\mathbf{m}_e$ can be written as

$$\mathbf{m}_e = \int_{V_e}\rho\mathbf{N}^T\mathbf{N}\mathrm{d}V = \int_{A_e} h\rho\mathbf{N}^T\mathbf{N}\mathrm{d}A \tag{14}$$

where ρ is the material density, h is the thickness of element, V_e and A_e is the volume and area of plane element, respectively. The non-mapped Lagrange shape function $\mathbf{N}(\mathbf{x})$ is used for calculating the shape function values. For quadrilateral element, the shape function is given by

$$\mathbf{N}(x,y) = [\,1 \quad x \quad y \quad xy\,] \begin{bmatrix} 1 & x_1 & y_1 & x_1y_1 \\ 1 & x_2 & y_2 & x_2y_2 \\ 1 & x_3 & y_3 & x_3y_3 \\ 1 & x_4 & y_4 & x_4y_4 \end{bmatrix}^{-1} = [\,1 \quad x \quad y \quad xy\,] \begin{bmatrix} a_{11} & a_{12} & a_{13} & a_{14} \\ a_{21} & a_{22} & a_{23} & a_{24} \\ a_{31} & a_{32} & a_{33} & a_{34} \\ a_{41} & a_{42} & a_{43} & a_{44} \end{bmatrix} \tag{15}$$

where $x_i, y_i (i = 1,2,3,4)$ are the global coordinates of nodes. $a_{ij} (i = 1,2,3,4 \quad j = 1,2,3,4)$ is the element of inverse matrix corresponding to global coordinates of nodes.

For the problems with uniform thickness and density, Eq. (14) can be rewritten as

$$\mathbf{m}_e = h\rho \int_{A_e} \mathbf{N}^T \mathbf{N} \mathrm{dA} = \begin{bmatrix} m_{11} & m_{12} & m_{13} & m_{14} \\ m_{21} & m_{22} & m_{23} & m_{24} \\ m_{31} & m_{32} & m_{33} & m_{34} \\ m_{41} & m_{42} & m_{43} & m_{44} \end{bmatrix} \tag{16}$$

and

$$m_{ij} = \begin{bmatrix} h\rho \int_{A_e} N_i N_j \mathrm{d}A & 0 \\ 0 & h\rho \int_{A_e} N_i N_j \mathrm{d}A \end{bmatrix} = \begin{bmatrix} \tilde{m}_{ij} & 0 \\ 0 & \tilde{m}_{ij} \end{bmatrix} \tag{17}$$

where

$$\tilde{m}_{ij} = h\rho \int_{A_e} N_i N_j \mathrm{d}A \tag{18}$$

And $N_i (i = 1,2,3,4)$ is the shape function of node i of quadrilateral element. From Eq. (14), we can obtain

$$N_i = a_{1i} + a_{2i}x + a_{3i}y + a_{4i}xy \tag{19}$$

$$N_i N_j = a_{1i}N_j + a_{2i}xN_j + a_{3i}yN_j + a_{4i}xyN_j \tag{20}$$

Appling the theorem of symbolic integration, the surface integral of Eq. (18) can be rewritten as line integral

$$\tilde{m}_{ij} = h\rho \int_{A_e} N_i N_j \mathrm{d}A = h\rho \int_{\Gamma} \left(\int N_i N_j \mathrm{d}x \right) n_1 \mathrm{d}\Gamma \tag{21}$$

and

$$\int N_i N_j \mathrm{d}x = (a_{1i} + a_{3i}y) \int N_j \mathrm{d}x + (a_{2i} + a_{4i}y) \int x N_j \mathrm{d}x \tag{22}$$

$$\int N_i \mathrm{d}x = a_{1i}x + \frac{1}{2}a_{2i}x^2 + a_{3i}yx + \frac{1}{2}a_{4i}x^2y \tag{23}$$

$$\int x N_i \mathrm{d}x = \frac{1}{2}a_{1i}x^2 + \frac{1}{3}a_{2i}x^3 + \frac{1}{2}a_{3i}x^2y + \frac{1}{3}a_{4i}x^3y \tag{24}$$

Using the Gauss integration, the integral of Eq. (21) can be evaluated by

$$\tilde{m}_{ij} = h\rho \int_{\Gamma} \left(\int N_i N_j \mathrm{d}x \right) n_1 \mathrm{d}\Gamma = h\rho \sum_{m=1}^{k} \sum_{n=1}^{N_G} \frac{1}{2} w_{m,n} \Phi_{ij} \left(x_{m,n}^{GP}, y_{m,n}^{GP} \right) n_1^m l_m \tag{25}$$

and

$$\Phi_{ij} \left(x_{m,n}^{GP}, y_{m,n}^{GP} \right) = \left(\int N_i N_j \mathrm{d}x \right) \Big|_{\left(x_{m,n}^{GP}, y_{m,n}^{GP} \right)} \tag{26}$$

Here, the integration of consistent mass matrix has been recast into line integral, which is convenient for us to implement the Gaussian quadrature. Moreover, it does not need to map the coordinates and to evaluate the Jacobian matrix.

4 Dynamic equations of SFEM

A 2D linear elastic dynamic problem with domain Ω is considered in this work, which subjects to body force $\mathbf{b}$, external applied traction $\tilde{\mathbf{T}}$ on the boundary Γ_t and displacement boundary condition $\mathbf{u} = \bar{\mathbf{u}}$ on Γ_u. The governing equation of dynamic problem can be obtained by using the principle of virtual displacement

$$\int_{\Omega} \delta\boldsymbol{\varepsilon}^{\mathrm{T}} \mathbf{D} \varepsilon \mathrm{d}\Omega - \int_{\Omega} \delta\mathbf{u}^{\mathrm{T}} [\mathbf{b} - \rho\ddot{\mathbf{u}} - \mathbf{c}\dot{\mathbf{u}}] \mathrm{d}\Omega - \int_{\Gamma_t} \delta\mathbf{u}^{\mathrm{T}} \tilde{\mathbf{T}} \mathrm{d}\Gamma = 0 \tag{27}$$

where $\boldsymbol{\varepsilon}$ is the strain matrix, $\mathbf{u}$ is the displacement tensor, $\delta\boldsymbol{\varepsilon}$ and $\delta\mathbf{u}$ is the virtual strain and virtual

displacement, respectively. **D** is the tensor of material constants. c is the damping coefficient.

According to the spatial discretization procedure of FEM, the Eq. (27) can be rewritten as

$$\begin{aligned}&\delta\mathbf{d}_\mathbf{e}^{\mathrm{T}}\int_{A_e} h\mathbf{B}^{\mathbf{T}}\mathbf{D}\mathbf{B}\mathbf{d}_\mathbf{e}\mathrm{d}A\\&-\delta\mathbf{d}_\mathbf{e}^{\mathrm{T}}\int_{A_e} h\mathbf{N}^{\mathrm{T}}\left[\mathbf{b}-\rho\mathbf{N}\ddot{\mathbf{d}}_\mathbf{e}-c\mathbf{N}\dot{\mathbf{d}}_\mathbf{e}\right]\mathrm{d}A\\&-\delta\mathbf{d}_\mathbf{e}^{\mathrm{T}}\int_{\Gamma_{te}} N\tilde{\mathbf{T}}\mathrm{d}\Gamma=0\end{aligned}\tag{28}$$

and

$$\delta\mathbf{u}_\mathbf{e}=\mathbf{N}\delta\mathbf{d}_\mathbf{e}=\sum_I N_I\delta\mathrm{d}_I,\qquad \mathbf{u}_\mathbf{e}=\mathbf{N}\mathbf{d}_\mathbf{e}=\sum_I N_I\mathrm{d}_I\tag{29}$$

$$\delta\boldsymbol{\varepsilon}_\mathbf{e}=\mathbf{B}\delta\mathbf{d}_\mathbf{e}=\sum_I \mathbf{B}_I\delta\mathrm{d}_I,\qquad \boldsymbol{\varepsilon}_\mathbf{e}=\mathbf{B}\mathbf{d}_\mathbf{e}=\sum_I \mathbf{B}_I\mathrm{d}_I\tag{30}$$

where $\mathbf{d}_I=[u_I\ \ v_I]^{\mathrm{T}}$ is the nodal displacement vector of element, and **B** is the strain matrix. For 2D linear elastic dynamic problems, the strain matrix can be expressed as

$$\mathbf{B}_I=\begin{bmatrix}\dfrac{\partial N_I}{\partial x} & 0 & \dfrac{\partial N_I}{\partial y}\\ 0 & \dfrac{\partial N_I}{\partial y} & \dfrac{\partial N_I}{\partial x}\end{bmatrix}^{\mathrm{T}}\tag{31}$$

Due to the arbitrary variation of displacements, the governing equation of element can be written as

$$\mathbf{k}_\mathbf{e}\mathbf{d}_\mathbf{e}+\mathbf{m}_e\ddot{\mathbf{d}}_\mathbf{e}+\mathbf{c}_\mathbf{e}\dot{\mathbf{d}}_\mathbf{e}=\mathbf{f}_\mathbf{e}\tag{32}$$

and

$$\mathbf{k}_\mathbf{e}=\int_{A_e} h\mathbf{B}^{\mathbf{T}}\mathbf{D}\mathbf{B}\mathrm{d}A\tag{33}$$

$$\mathbf{m}_e=\int_{A_e} h\mathbf{N}^{\mathrm{T}}\rho\mathbf{N}\mathrm{d}A\tag{34}$$

$$\mathbf{c}_\mathbf{e}=\int_{A_e} h\mathbf{N}^{\mathrm{T}}c\mathbf{N}\mathrm{d}A\tag{35}$$

$$\mathbf{f}_\mathbf{e}=\int_{A_e} h\mathbf{N}^{\mathrm{T}}\mathbf{b}\mathrm{d}A+\int_{\Gamma_t}\mathbf{N}\tilde{\mathbf{T}}\mathrm{d}\Gamma\tag{36}$$

where $\mathbf{k}_\mathbf{e}$, $\mathbf{m}_e$ and $\boldsymbol{\eta}_\mathbf{e}$ is the stiffness, mass and damp matrix of element, separately. $\mathbf{f}_\mathbf{e}$ is the element force vector.

In the SFEM, the strain matrix in Eq. (31) is calculated by strain smoothing operation [15]. The strain of an arbitrary point $\mathbf{x}_C$ can be written as the divergence of a spatial average of standard strain field

$$\tilde{\varepsilon}_\mathbf{e}(\mathbf{x}_C)=\int_{\Omega_C}\boldsymbol{\varepsilon}_\mathbf{e}(\mathbf{x})\phi(\mathbf{x}-\mathbf{x}_C)\mathrm{d}\Omega\tag{37}$$

where Ω_C may be an entire element or part of an element. $\phi(\mathbf{x}-\mathbf{x}_C)$ is the smoothing function and defined as

$$\phi(\mathbf{x}-\mathbf{x}_C)=\begin{cases}1/A_C, & x\in\Omega_C\\ 0, & x\notin\Omega_C\end{cases}\tag{38}$$

where $A_C=\int_{\Omega_C}\mathrm{d}\Omega$ is the area of smoothing cell Ω_C in the element Ω_e. The subdivision of smoothing cells in the element can be found in the Ref. [2].

Substituting ϕ and $\boldsymbol{\varepsilon}_\mathbf{e}$ into Eq. (37), the following equation can be obtained

$$\tilde{\varepsilon}_\mathbf{e}(\mathbf{x}_C)=\int_{\Omega_C}\mathbf{B}\mathbf{d}_\mathbf{e}\phi(\mathbf{x}-\mathbf{x}_C)\mathrm{d}\Omega=\tilde{\mathbf{B}}_\mathbf{C}\mathbf{d}_\mathbf{e}\tag{39}$$

where the smoothed matrix $\tilde{\mathbf{B}}_\mathbf{C}$ is defined by

$$\tilde{\mathbf{B}}_C=\frac{1}{A_C}\int_{\Omega_C}\mathbf{B}(\mathbf{x})\mathrm{d}\Omega\tag{40}$$

Substituting Eq. (31) into $\tilde{\mathbf{B}}_C$, the term of $\tilde{\mathbf{B}}_{IC}$ can be written as

$$\tilde{\mathbf{B}}_{IC}=\frac{1}{A_C}\int_{\Omega_C}\begin{bmatrix}\dfrac{\partial N_I}{\partial x} & 0 & \dfrac{\partial N_I}{\partial y}\\ 0 & \dfrac{\partial N_I}{\partial y} & \dfrac{\partial N_I}{\partial x}\end{bmatrix}^{\mathrm{T}}\mathrm{d}\Omega\tag{41}$$

Equation (41) can be changed by applying the divergence theorem to the smoothing cell Ω_C and their boundary $\Gamma_C=\partial\Omega_C$, which is rewritten as

$$\begin{aligned}\tilde{\mathbf{B}}_{IC}(\mathbf{x}_C)&=\frac{1}{A_C}\int_{\Gamma_C}\begin{bmatrix}n_xN_I & 0 & n_yN_I\\ 0 & n_yN_I & n_xN_I\end{bmatrix}^{\mathrm{T}}\mathrm{d}\Gamma\\&=\begin{bmatrix}\tilde{b}_{I1}(\mathbf{x}_C) & 0 & \tilde{b}_{I2}(\mathbf{x}_C)\\ 0 & \tilde{b}_{I2}(\mathbf{x}_C) & \tilde{b}_{I1}(\mathbf{x}_C)\end{bmatrix}^{\mathrm{T}}\end{aligned}\tag{42}$$

where $\mathbf{n}=(n_x,n_y)$ is the outward unit normal, and

$$\tilde{b}_{Ii}(\mathbf{x}_C) = \frac{1}{A_C}\int_{\Gamma_C} n_i(\mathbf{x}) N_I(\mathbf{x}) \mathrm{d}\Gamma \tag{43}$$

The integral in Eq. (43) can be evaluated by the Gaussian integration along each segment of boundary Γ_C of Ω_C, Eq. (43) is transformed to algebraic form

$$\tilde{b}_{Ii}(\mathbf{x}_C) = \frac{1}{A_C}\sum_{m=1}^{k}\sum_{n=1}^{N_G}\frac{1}{2} w_{m,n} n_i^m N_I\left(\mathbf{x}_{m,n}^{GP}\right) l_m \quad (i = 1, 2) \tag{44}$$

where $\mathbf{x}_{m,n}^{GP}$ is the integral point (Gaussian point) of boundary segment of Γ_C, whose length and outward unit normal are denoted as l_m and n^m, respectively.

Then, the stiffness matrix of SFEM is expressed as

$$\mathbf{k}_{\mathrm{e}} = \int_{A_e} h\mathbf{B}^{\mathbf{T}}\mathbf{D}\mathbf{B}\mathrm{d}A = \sum_{C=1}^{\mathrm{SC}}\int_{A_C} h\tilde{\mathbf{B}}_C^{\mathbf{T}}\mathbf{D}\tilde{\mathbf{B}}_C\mathrm{d}A \tag{45}$$

where SC is the number of smoothing cells that an element is subdivided, and $A_e = \sum_{C=1}^{\mathrm{SC}} A_C$. When the element is uniform thickness, the integral term of smoothing domain is constant, then Eq. (45) can be rewritten as

$$\mathbf{k}_{\mathrm{e}} = \sum_{C}^{\mathrm{SC}} A_C h\tilde{\mathbf{B}}_C^{\mathbf{T}}\mathbf{D}\tilde{\mathbf{B}}_C \tag{46}$$

Incorporating the novel integration scheme of consistent mass matrix into the SFEM formulation and assembling all the element matrices, the global system equation can be obtained by

$$\tilde{\mathbf{K}}\mathbf{d} + \tilde{\mathbf{M}}\ddot{\mathbf{d}} + C\dot{\mathbf{d}} = \mathbf{F} \tag{47}$$

where $\tilde{\mathbf{K}}$ is the smoothed global stiffness matrix, $\tilde{\mathbf{M}}$ is the global consistent mass matrix obtained by the novel integration scheme, $\mathbf{C}$ is the global damp matrix obtained as the same with global consistent mass matrix, $\mathbf{d}$ is the vector of displacements of all the nodes in the entire problem domain. $\mathbf{F}$ is the equivalent nodal force vector.

For free vibration analysis, the damping and external forces are set equal to zero. Then, the discretized system Eq. (47) becomes

$$\tilde{\mathbf{K}}\mathbf{d} + \tilde{\mathbf{M}}\ddot{\mathbf{d}} = \mathbf{0} \tag{48}$$

Generally, the solution of Eq. (48) can be assumed as

$$\mathbf{d} = \bar{\mathbf{d}}\exp(i\omega t) \tag{49}$$

where $\bar{\mathbf{d}}$ is the eigenvector, ω is the frequency and t is the time. By substituting Eq. (49) into (48), we obtain

$$\left(\tilde{\mathbf{K}} - \omega^2\tilde{\mathbf{M}}\right)\bar{\mathbf{d}} = \mathbf{0} \tag{50}$$

For forced vibration analysis with constant damping coefficient c, the damping matrix of Eq. (47) can be rewritten as

$$\tilde{\mathbf{C}}_{\mathbf{e}} = \int_{A_e} h\mathbf{N}^{\mathrm{T}}\mathrm{c}\mathbf{N}\mathrm{d}A = h\mathrm{c}\int_{A_e}\mathbf{N}^{\mathrm{T}}\mathbf{N}\mathrm{d}A \tag{51}$$

It can be found in Eq. (51) that the evaluation of domain integral can be easily recast into line integral as the procedure of mass matrix.

The Newmark's method [25] is used to solve the dynamic Eq. (47) in this paper. The formulations of Newmark's method are

$$\mathbf{u}_{t+\Delta t} = \mathbf{u} + \Delta t\dot{\mathbf{u}}_t + \left(\frac{1}{2} - \delta\right)\Delta t^2\ddot{\mathbf{u}}_t + \delta\Delta t^2\ddot{\mathbf{u}}_{t+\Delta t} \tag{52}$$

$$\dot{\mathbf{u}}_{t+\Delta t} = \dot{\mathbf{u}}_t + (1-\eta)\Delta t\ddot{\mathbf{u}}_t + \eta\Delta t\ddot{\mathbf{u}}_{t+\Delta t} \tag{53}$$

where δ and η are parameters determined by stability and integral accuracy. Δt is the time increment. Substituting Eqs. (52) and (53) into Eq. (47), the dynamic response at time $t + \Delta t$ can be obtained.

The Newmark's method is unconditionally stable, if

$$\eta \geq 0.5 \quad \text{and} \quad \delta \geq \frac{1}{4}(\eta + 0.5)^2 \tag{54}$$

In this work, $\eta = 0.5$, $\delta = 0.25$ are used.

In present work, the four-node quadrilateral (Q4) element and cell-based strain smoothing operation are used for numerical implementation. Four quadrilateral smoothing cells (SC = 4) are divided to calculate the integral of Q4 element. In order to investigate the influence of irregular meshes on numerical results, the irregular meshes can be constructed by the following equations

$$\begin{cases} x' = x + r_c\alpha\Delta x \\ y' = y + r_c\alpha\Delta y \end{cases} \tag{55}$$

where x, y are the initial coordinates of nodes of regular meshes, x', y' are the new coordinates of nodes of irregular meshes. r_c is a random number from -1 to 1, and α is a prescribed irregularity factor whose value is chosen from 0 to 0.5. Δx and Δy is the element size

in x- and y-directions of the initial regular mesh, respectively [2]. In present work, the irregular elements with $\alpha = 0.1, 0.2, 0.3, 0.4$ are adopted to compare with the regular elements.

5 Numerical examples

5.1 Free vibration analysis

In this numerical example, a cantilever beam, as shown in Fig. 1, is analyzed as a free vibration problem. The dimensionless parameters taken in the computation are length $L = 48$, height $H = 12$, thickness $h = 1.0$, Young's modulus $E = 3.0 \times 10^7$, Possion's ratio $v = 0.3$, mass density $\rho = 1$. Figure 2 is the typical regular meshes of cantilever beam for analysis.

The eigenvalues are investigated in this example. Table 1 lists the natural frequencies obtained by different number of regular meshes. Two Gaussian points are used for each boundary segment of smoothing cells in the present method. The results obtained by SFEM and FEM are also listed in Table 1, in which the traditional consistent mass matrix is adopted for the calculation of SFEM. It can be observed in Table 1 that the results obtained by present method are the same as those of SFEM, and it indicates that the novel integration scheme of consistent mass matrix, which no coordinate mapping is required, possesses the same accuracy as the traditional consistent mass matrix. Because in the calculation of FEM, the lumped mass matrix overestimates the mass effect and the consistent mass matrix underestimates the mass effect [17], the exact natural frequencies should be located in the interval of results obtained by FEM with lumped mass matrix and those with consistent mass matrix. Hence, it can be confirmed that the results given by present method are close to the exact solutions, see from Table 1. The first to ninth eigenmodes obtained by present method are plotted in Fig. 3. The results shown in Fig. 3 are consistent with those given in Ref. [23, 24].

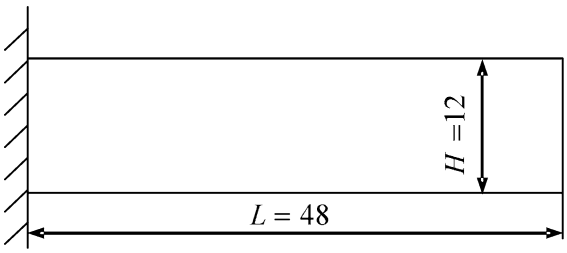

Fig. 1 Cantilever beam for free vibration analysis

In order to investigate the influence of the number of Gaussian integral points, which are used for each boundary segment of smoothing cells, on the accuracy of present method, the results of first to ninth eigenmodes of the cantilever beam are listed in Table 2, in which 20×8 elements are used for analysis. The number of Gaussian integral points to be used depends on the complexity of the integrand, and the use of m Gaussian integral points gives the exact results of a polynomial integrand of up to order of $n = 2m - 1$. In this case, it can be observed from Table 2 that two Gaussian points are enough to obtain the stable and accurate results in this numerical example.

Due to the strain smoothing technique for stiffness matrix and the novel integration scheme for mass matrix, one of the advantages of the present method is that the numerical accuracy can be maintained for irregular meshes. Figure 4 shows the 20×8 irregular elements with $\alpha = 0.4$. Table 3 gives the results of first to fifth natural frequencies of the cantilever beam obtained by different irregular elements. It can be seen that the good stable and accurate results are also obtained by present method with different irregular meshes.

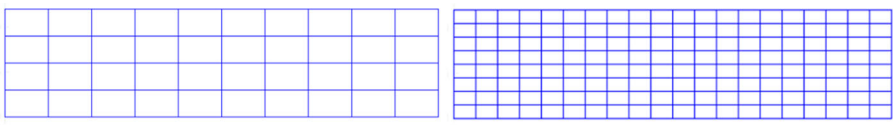

Fig. 2 Typical regular meshes of the cantilever beam. **a** Number of elements: 10×8, **b** number of elements: 20×8

Table 1 The natural frequencies obtained by different mesh distributions

Mode	10 × 4 elements				20 × 8 elements				40 × 16 elements				FEM (4850 DOF)	
	Present method	SFEM	FEM		Present method	SFEM	FEM		Present method	SFEM	FEM			
			Lumped mass	Consistent mass			Lumped mass	Consistent mass			Lumped mass	Consistent mass	Lumped mass	Consistent mass
1	28.31	28.31	28.60	28.74	27.88	27.88	27.76	27.99	27.75	27.75	27.78	27.79	27.72	27.73
2	146.45	146.45	144.12	148.23	142.29	142.29	141.79	142.78	141.19	141.19	141.07	141.32	140.86	140.92
3	180.10	180.10	179.77	180.15	179.82	179.82	179.82	179.84	179.74	179.74	179.72	179.75	179.71	179.71
4	344.85	344.85	328.47	348.49	329.11	329.11	328.01	330.14	325.04	325.04	324.09	325.31	323.89	324.01
5	542.58	542.58	523.36	542.90	535.96	535.96	534.23	537.57	526.14	526.14	523.09	526.58	523.43	523.62
6	574.50	574.50	532.41	579.87	538.09	538.09	538.08	538.19	536.91	536.91	536.29	536.95	536.57	536.59
7	825.05	825.05	716.35	831.64	753.60	753.60	751.15	755.84	735.13	735.13	728.45	735.75	730.04	730.34
8	907.62	907.62	859.23	909.28	887.72	887.72	887.69	888.22	882.70	882.70	879.69	882.84	881.28	881.35
9	969.49	969.49	875.84	971.78	921.78	921.78	920.36	923.07	904.65	904.65	897.23	905.09	899.69	899.88
10	1102.67	1102.67	956.34	1108.51	1025.07	1025.07	1022.78	1027.19	1005.30	1005.30	996.50	1005.85	1000.22	1000.46

5.2 Forced vibration analysis

In this example, a cantilever beam subjected to a dynamic force $P = 1000g(t)$ at the right end is used for forced vibration analysis. $g(t)$ is a function of time to represent the dynamic loading. The geometrical parameters and material parameters are the same as those of Sect. 5.1. Three types of dynamic loading are implemented for analysis, including simple harmonic loading, constant loading and transient loading. The cantilever beam model and different dynamic loading are given in Fig. 5.

In the case of harmonic loading, a simple harmonic load $g(t) = \sin(\omega t)$ is used, as shown in Fig. 5b. ω is the frequency of dynamic load, and $\omega = 27$ is used in this example. The damping is neglected in this case. The dynamic responses at point A obtained by the present method are shown in Fig. 6. Different time increments are employed with 20 × 8 elements to investigate the robustness of time increment for dynamic analysis. It can be seen from Fig. 6 that the good results can be obtained when $\Delta t \leq 0.01$. The time increment $\Delta t = 0.005$ will be employed in the following calculation. Figure 7 shows the results obtained by present method with different irregular elements. The present results compared with SFEM and FEM are shown in Fig. 8. It is observed that the numerical accuracy of present method can maintain even for extremely distorted meshes. However, the accuracy of FEM is poor when irregular meshes with $\alpha = 0.4$ are used.

When the dynamic loading is constant $g(t) = 1.0$, as shown in Fig. 5c, it can be taken as a dynamic relaxation to check the stability and efficiency of present numerical method [23]. If the damping is neglected, the response of this problem is stable vibration with the static deformation, and the displacement at point A can be obtained by analytical solution [26]. When the damping is considered, the response will converge to the static deformation. In this case, 40 × 16 elements with different irregular factors are implemented. The damping coefficient is c = 0.4. Table 4 demonstrates the results obtained in the stage of convergence, in which the results obtained by SFEM, FEM and Ref. [23] are included for comparative study. It can be found that the stable and accurate results can be obtained by present method even though the severely irregular meshes are used. The results of present method are almost the same as those of SFEM,

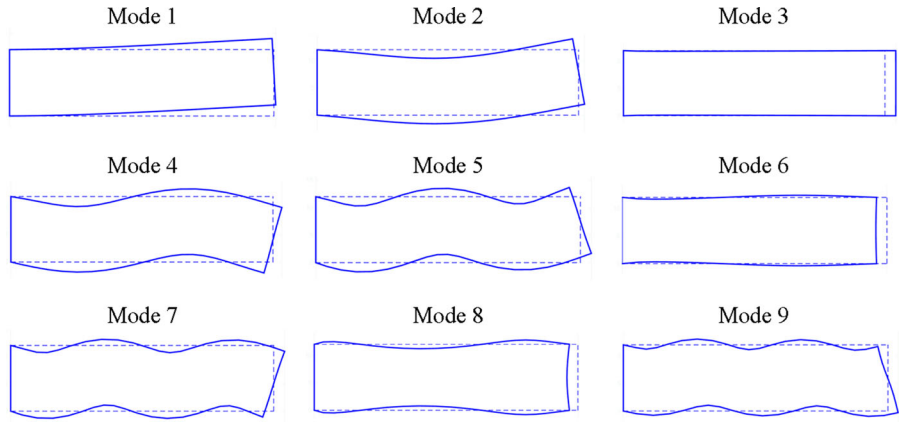

Fig. 3 First to ninth eigenmodes of the cantilever beam

Table 2 First to fifth natural frequencies of cantilever beam by using different number of Gaussian points

Mode	Number of Gaussian points				
	1	2	3	4	5
1	27.88	27.88	27.88	27.88	27.88
2	142.32	142.29	142.29	142.29	142.29
3	179.82	179.82	179.82	179.82	179.82
4	329.21	329.11	329.11	329.11	329.11
5	536.19	535.96	535.96	535.96	535.96

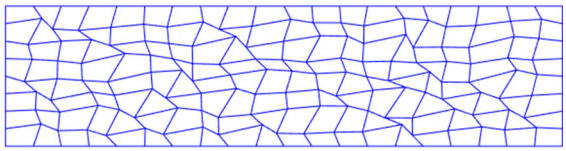

Fig. 4 Irregular elements with $\alpha = 0.4$ (20 × 8 elements)

Table 3 First to fifth natural frequencies of the cantilever beam by using irregular elements (20 × 8 elements)

Mode	$\alpha = 0$	$\alpha = 0.1$	$\alpha = 0.2$	$\alpha = 0.3$	$\alpha = 0.4$
1	27.88	27.88	27.84	27.80	27.84
2	142.29	142.29	142.12	142.22	142.24
3	179.82	179.73	179.41	178.79	178.14
4	329.11	329.09	329.08	330.25	328.14
5	535.96	536.22	536.11	535.81	534.06

but are more accurate than those of FEM and Ref. [23]. Furthermore, the calculation of FEM is invalid when the extremely irregular meshes with $\alpha = 0.4$ are used.

Figure 9 is the dynamic responses at point A obtained by present method, it can be seen that the good stable results are obtained by different irregular elements.

In the following, the cantilever beam subjected to a transient loading is investigated, as shown in Fig. 5d, the loading function in this case is given as

$$g(t) = \begin{cases} 1 & 0 \le t \le 0.5 \\ 0 & t > 0.5 \end{cases} \tag{56}$$

In this computation, 20 × 8 elements are used. Figures 10 and 11 are the dynamic responses at point A without damping. Figures 12 and 13 are the results with damping c = 0.4. The results obtained by different irregular elements are also given in these figures. It can be seen that good stability and accuracy can also be obtained by the present method for forced vibration analysis. However, as shown in Figs. 11 and 13, the results of FEM are sensitive to irregular meshes and the accuracy of results is poor for $\alpha = 0.4$.

6 Conclusions

The symbolic integration combining indefinite integral with Gauss divergence theorem has been employed to form a novel integration scheme for consistent mass matrix of FEM. Then the novel integration scheme of consistent mass matrix is incorporated into SFEM for solving 2D linear elastic dynamic problems. Comparing with the conventional FEM, no coordinate mapping is required for consistent mass matrix and damping matrix. From the results illustrated in several numerical examples, it can also be concluded that the present

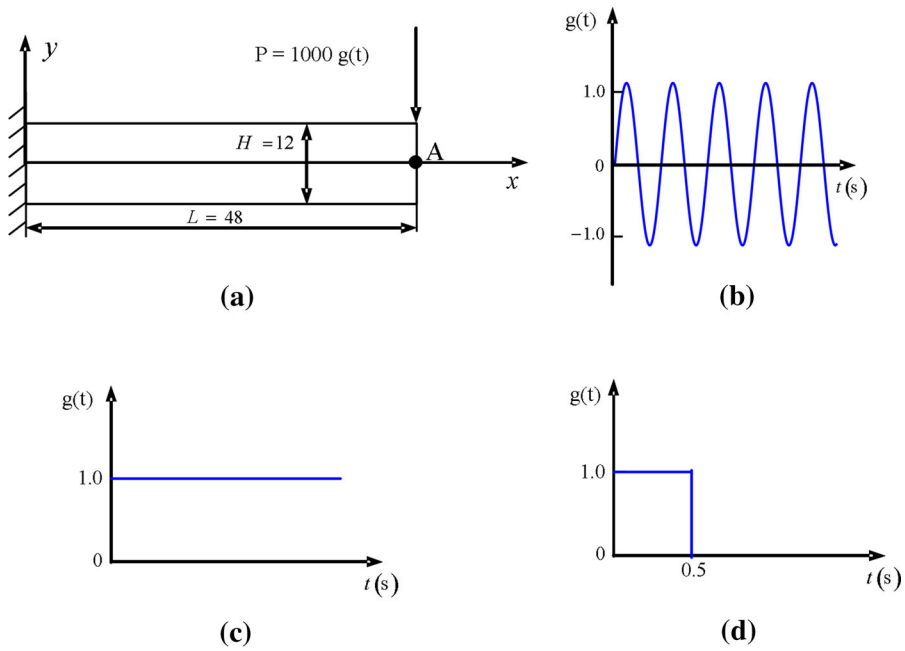

Fig. 5 Cantilever beam for forced vibration analysis. **a** Cantilever beam, **b** harmonic loading, **c** constant loading, **d** transient loading

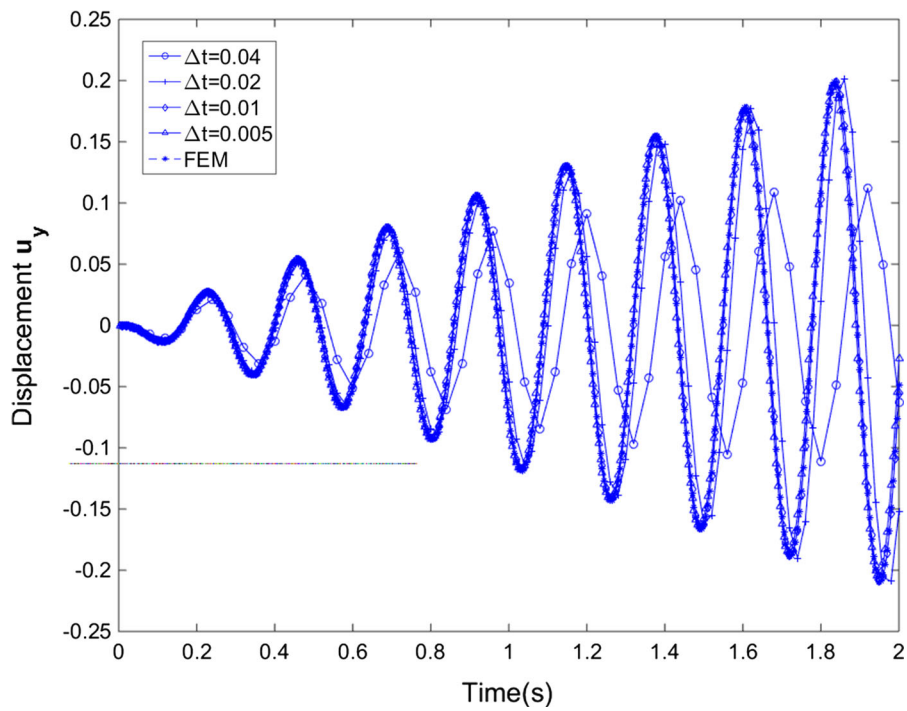

Fig. 6 Responses at point A without damping under harmonic load with different time increments

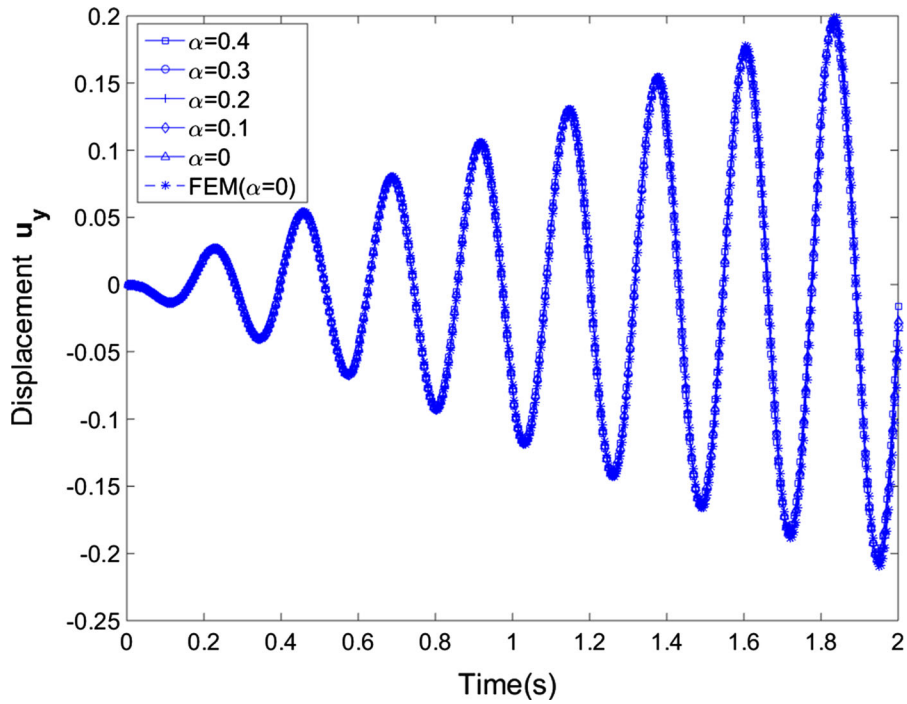

Fig. 7 Responses at point A without damping under harmonic load by present method with irregular elements

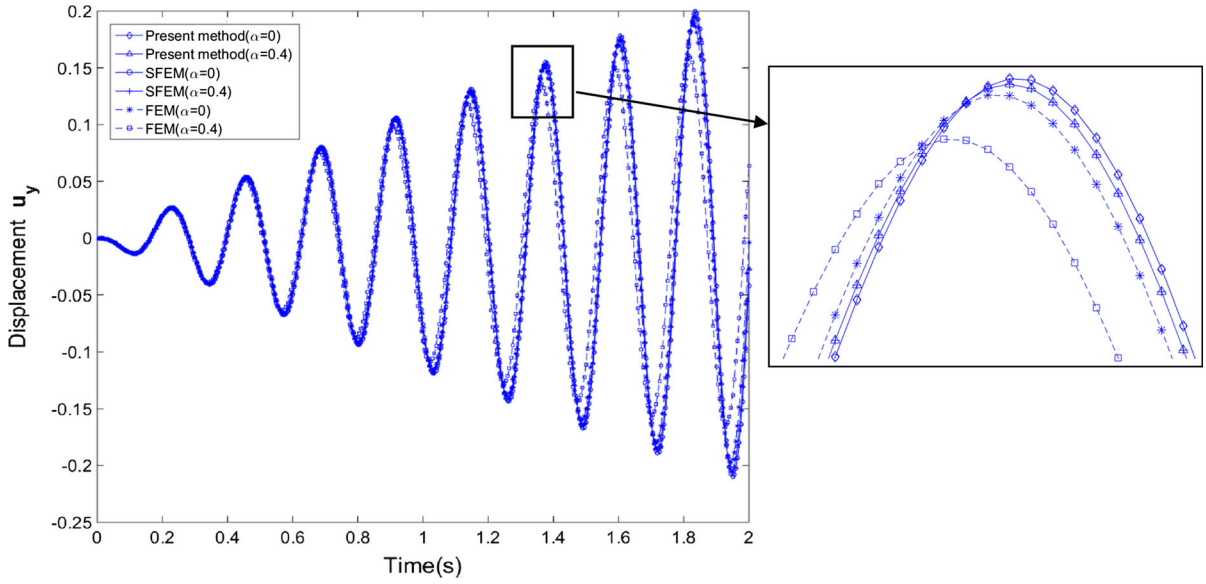

Fig. 8 Responses at point A without damping under harmonic load by different methods with irregular elements

method can obtain accurate results as well as conventional FEM, moreover, the present method can maintain the numerical accuracy even the severely irregular elements are used.

Benefit from the novel integration scheme, it can be forecasted that the integral of matrices of FEM evaluated along the boundary of smoothing cells can be taken as a robust technique for numerical

Table 4 Results obtained by different irregular elements under constant loading ($t = 50$ s)

	Displacement u_y (exact: $u_y = -0.0089$)				
	$\alpha = 0$	$\alpha = 0.1$	$\alpha = 0.2$	$\alpha = 0.3$	$\alpha = 0.4$
Present method	−0.008866	−0.008877	−0.008896	−0.008956	−0.009087
SFEM	−0.008866	−0.008875	−0.008915	−0.008981	−0.009087
FEM	−0.008846	−0.008844	−0.008829	−0.008806	–
Ref. [23]	−0.008842				

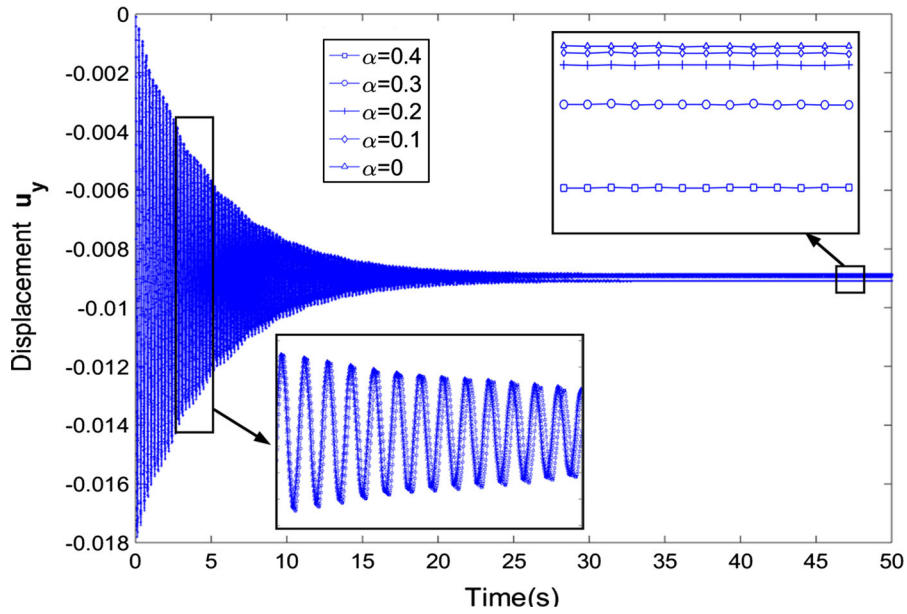

Fig. 9 Responses at point A with damping under constant loading

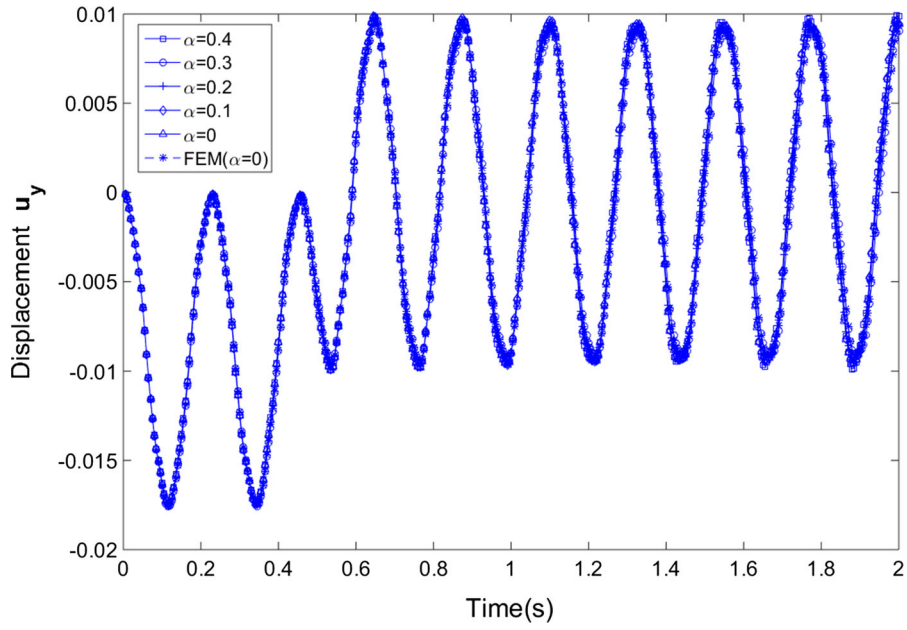

Fig. 10 Responses at point A without damping under transient loading obtained by present method

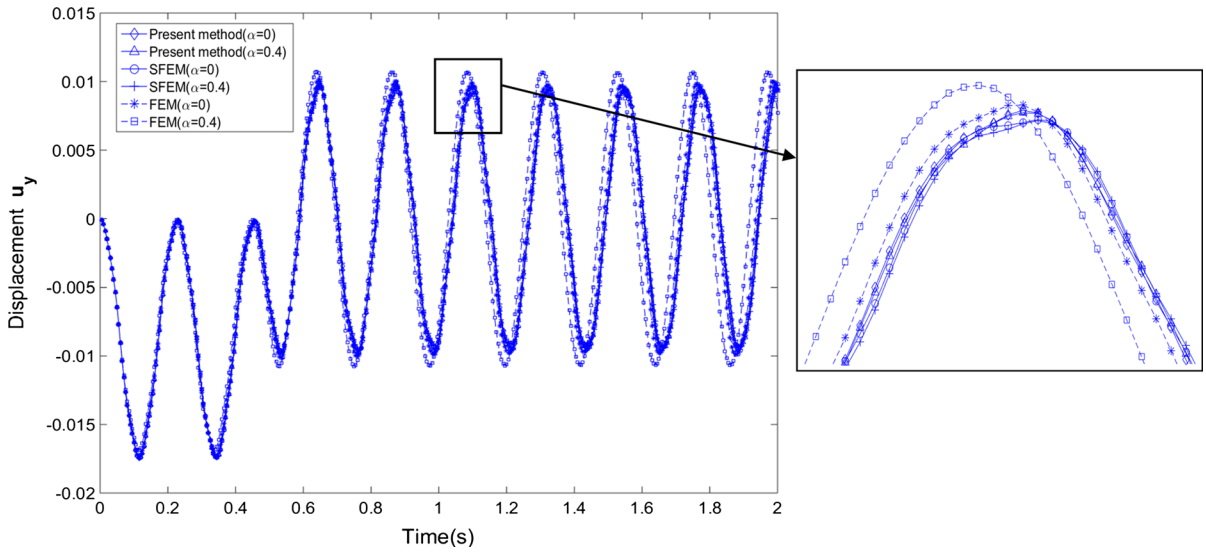

Fig. 11 Responses at point A without damping under transient loading obtained by different methods

Fig. 12 Responses at point A with damping under transient loading obtained by present method

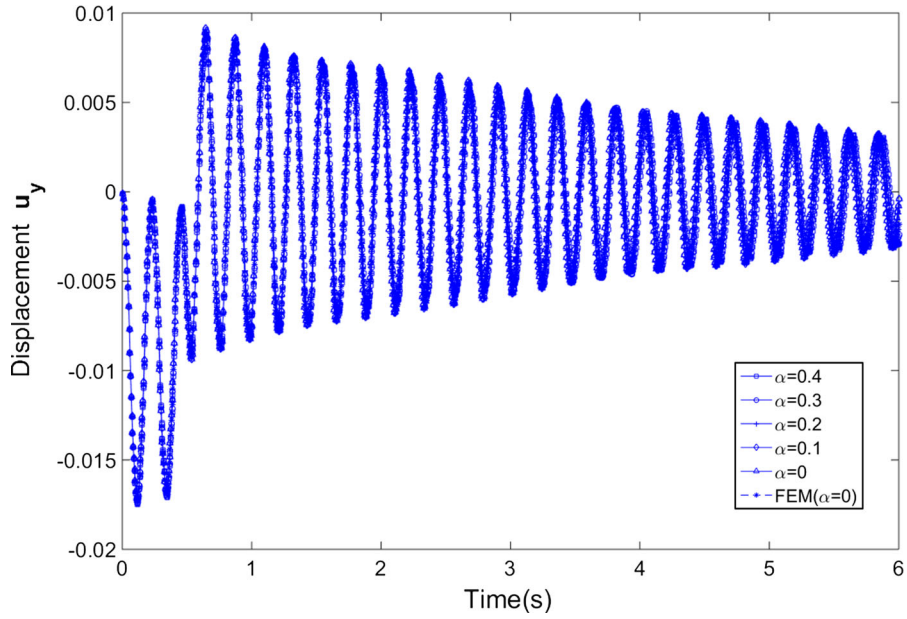

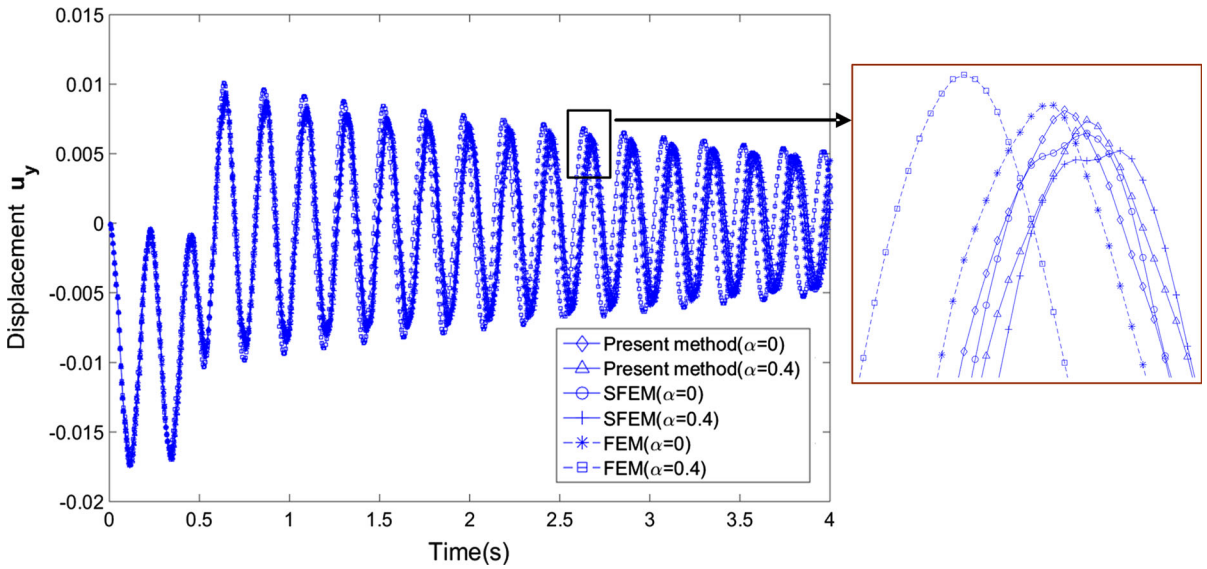

Fig. 13 Responses at point A with damping under transient loading obtained by different methods

simulation. It is also easily extended the present integration scheme to solve the matrices of FEM which contain non partial derivative terms of shape function, such as in the problems of plate, shell and etc.

Acknowledgments Financial supports from National Natural Science Foundation of China (11372106, 11272118) are gratefully acknowledged.

References

1. Zienkiewicz OC, Taylor RL (2000) The finite element method, 5th edn. Butterworth, Heinemann, Oxford
2. Liu GR, Dai KY, Nguyen TT (2007) A smoothed finite element method for mechanics problems. Comput Mech 39(6):859–877
3. Chen JS, Wu CT, Yoon S et al (2001) A stabilized conforming nodal integration for Galerkin mesh-free methods. Int J Numer Meth Eng 50(2):435–466
4. Liu GR, Nguyen-Xuan H, Nguyen-Thoi T (2010) A theoretical study on the smoothed FEM (S-FEM) models: properties, accuracy and convergence rates. Int J Numer Meth Eng 84(10):1222–1256
5. Bordas SPA, Rabczuk T, Hung NX et al (2010) Strain smoothing in FEM and XFEM. Comput Struct 88(23): 1419–1443
6. Nguyen-Thoi T, Vu-Do HC, Rabczuk T et al (2010) A node-based smoothed finite element method (NS-FEM) for upper bound solution to visco-elastoplastic analyses of solids using triangular and tetrahedral meshes. Comput Methods Appl Mech Eng 199(45):3005–3027
7. Liu GR, Chen L, Nguyen-Thoi T et al (2010) A novel singular node-based smoothed finite element method (NS-FEM) for upper bound solutions of fracture problems. Int J Numer Meth Eng 83(11):1466–1497
8. Nguyen-Xuan H, Liu GR, Nguyen-Thoi T et al (2009) An edge-based smoothed finite element method for analysis of two-dimensional piezoelectric structures. Smart Mater Struct 18(6):065015
9. Liu GR, Nguyen-Thoi T, Lam KY (2009) An edge-based smoothed finite element method (ES-FEM) for static, free and forced vibration analyses of solids. J Sound Vib 320(4):1100–1130
10. Phan-Dao HH, Nguyen-Xuan H, Thai-Hoang C et al (2013) An edge-based smoothed finite element method for analysis of laminated composite plates. Int J Comput Methods 10(01):1340005
11. Luong-Van H, Nguyen-Thoi T, Liu GR et al (2014) A Cell-based smoothed Finite Element Method using Mindlin plate element (CS-FEM-MIN3) for dynamic response of composite plates on viscoelastic foundation. Eng Anal Bound Elem 42:8–19
12. Nguyen-Thoi T, Phung-Van P, Thai-Hoang C et al (2013) A cell-based smoothed discrete shear gap method (CS-DSG3) using triangular elements for static and free vibration analyses of shell structures. Int J Mech Sci 74:32–45
13. Chen L, Rabczuk T, Bordas SPA et al (2012) Extended finite element method with edge-based strain smoothing (ESm-XFEM) for linear elastic crack growth. Comput Methods Appl Mech Eng 209:250–265
14. Liu P, Bui TQ, Zhang C et al (2012) The singular edge-based smoothed finite element method for stationary dynamic crack problems in 2D elastic solids. Comput Methods Appl Mech Eng 233:68–80
15. Dai KY, Liu GR (2007) Free and forced vibration analysis using the smoothed finite element method (SFEM). J Sound Vib 301(3):803–820

16. Nguyen-Thoi T, Phung-Van P, Rabczuk T T et al (2013) Free and forced vibration analysis using the n-sided polygonal cell-based smoothed finite element method (nCS-FEM). Int J Comput Methods 10(01):1340008
17. Kim K (1993) A review of mass matrices for eigenproblems. Comput Struct 46(6):1041–1048
18. Wu SR (2006) Lumped mass matrix in explicit finite element method for transient dynamics of elasticity. Comput Methods Appl Mech Eng 195(44):5983–5994
19. Cohen G, Joly P, Tordjman N (1994) Higher-order finite elements with mass-lumping for the 1D wave equation. Finite Elem Anal Des 16(3):329–336
20. Babuška I, Osborn J (1991) Eigenvalue problems. Handb Numer Anal 2:641–787
21. Dasgupta G (2003) Integration within polygonal finite elements. J Aerosp Eng 16(1):9–18
22. Thiagarajan V, Shapiro V (2014) Adaptively weighted numerical integration over arbitrary domains. Comput Math Appl 67(9):1682–1702
23. Li H, Wang QX, Lam KY (2004) Development of a novel meshless Local Kriging (LoKriging) method for structural dynamic analysis. Comput Methods Appl Mech Eng 193(23):2599–2619
24. Wang Y, Hu D, Yang G et al (2015) An effective subdomain smoothed Galerkin method for free and forced vibration analysis. Meccanica 50(5):1285–1301
25. Belytschko T (1983) An overview of semidiscretization and time integration procedures. In: Computational methods for transient analysis. Amsterdam, North-Holland, pp 1–65
26. Timoshenko SP, Goodier JN (1970) Theory of elasticity, 3rd edn. McGraw-Hill, New York